The Transcriptional Repressor dMnt Is a Regulator of Growth in *Drosophila melanogaster*

Lenora W. M. Loo, Julie Secombe, John T. Little, Leni-Sue Carlos, Cynthia Yost, Pei-Feng Cheng, Erin M. Flynn, Bruce A. Edgar and Robert N. Eisenman

Mol. Cell. Biol. **2005, 25(16):7078. DOI: 10.1128/MCB.25.16.7078-7091.2005.**

MOLECULAR AND CELLULAR BIOLOGY, Aug. 2005, p. 7078–7091 Vol. 25, No. 16
0270-7306/05/$08.00+0 doi:10.1128/MCB.25.16.7078–7091.2005

The Transcriptional Repressor dMnt Is a Regulator of Growth in *Drosophila melanogaster*†

Lenora W. M. Loo,‡ Julie Secombe,‡ John T. Little, Leni-Sue Carlos, Cynthia Yost, Pei-Feng Cheng, Erin M. Flynn, Bruce A. Edgar, and Robert N. Eisenman*

Division of Basic Sciences, Fred Hutchinson Cancer Research Center, Seattle, Washington

Received 4 May 2005/Returned for modification 22 May 2005/Accepted 27 May 2005

The Myc-Max-Mad/Mnt network of transcription factors has been implicated in oncogenesis and the regulation of proliferation in vertebrate cells. The identification of Myc and Max homologs in *Drosophila melanogaster* has demonstrated a critical role for dMyc in cell growth control. In this report, we identify and characterize the third member of this network, dMnt, the sole fly homolog of the mammalian Mnt and Mad family of transcriptional repressors. dMnt possesses two regions characteristic of Mad and Mnt proteins: a basic helix-loop-helix-zipper domain, through which it dimerizes with dMax to form a sequence-specific DNA binding complex, and a Sin-interacting domain, which mediates interaction with the dSin3 corepressor. Using the upstream activation sequence/GAL4 system, we show that expression of dMnt results in an inhibition of cellular growth and proliferation. Furthermore, we have generated a dMnt null allele, which results in flies with larger cells, increased weight, and decreased life span compared to wild-type flies. Our results demonstrate that dMnt is a transcriptional repressor that regulates *D. melanogaster* body size.

The Myc-Max-Mad/Mnt network is comprised of a group of conserved transcription factors of the basic helix-loop-helix-zipper (bHLHZ) class which are thought to function together as a molecular module (24) to transcriptionally regulate cell growth, proliferation, and differentiation (for recent reviews, see references 5, 17, 21, 37, 49, and 77). The bHLHZ domains common to these transcription factors mediate dimerization of Myc or Mad family proteins with Max, thereby permitting Myc-Max and Mad-Max heterodimer binding to the E-box sequence CACGTG. An important aspect of the network is that it is capable of transcriptional activation and repression of multiple gene targets through recruitment of chromatin-modifying complexes. Myc associates with the coactivators TRRAP (40, 41) and p300/CBP (73), which bind or possess histone acetyltransferase activities. Histone acetyltransferase recruitment is generally associated with augmented gene expression (2, 23). In contrast, Mad and Mnt family proteins associate with the Sin3 corepressor, which recruits histone deacetylases, leading to transcriptional repression (for reviews, see references 39 and 77). Myc-Max complexes have also been shown to repress the expression of several genes indirectly by binding and inactivating the Miz-1 transcription factor (64–66).

Much research has focused on mammalian Mad family proteins and Mnt, since they appear to antagonize Myc activity and could function, at least in principle, as tumor suppressors. The mammalian Mad family of transcriptional repressors is encoded by four paralogs: *mad1*, *mxi1*, *mad3*, and *mad4* (reviewed in reference 39). The other characterized Max-binding repressor, Mnt (also known as Rox), possesses the two conserved domains common to all Mad family members: the N-terminal Sin-interacting domain (SID), which interacts with the Sin3 corepressor, and the bHLHZ domain required for heterodimerization with Max (26, 42). However, Mnt is considerably larger than any of the Mad family proteins and contains other regions, including proline- and proline/histidine-rich sequences, that are unique to Mnt.

Attempts to understand the physiological roles of mammalian Mad and Mnt proteins have entailed both overexpression and targeted gene deletion studies. In general, this work has provided support for the notion that Mad and Mnt antagonize Myc function and promote cell cycle exit (12, 13, 20, 28, 33, 34, 55, 59, 74).

Surprisingly, given the capacity for overexpressed *mad* to inhibit proliferation, targeted deletions of *mad* family genes in mice did not result in dramatic phenotypes relating to differentiation and development. Mice homozygous for a *mad1* null mutation displayed no detectable differences in viability, fertility, size, behavior, or incidence of neoplasia compared to controls. However, their granulocyte progenitor cells, when cultured in vitro, exhibited a delay in differentiation due to an inhibition of cell cycle exit (18). *mxi1* knockout mice showed generalized hyperplasia in certain tissues and an increased incidence of carcinogen-induced tumors in older animals (62). The only detectable phenotype in *mad3* homozygous null mice was an increased sensitivity to gamma irradiation in neural progenitor cells and thymocytes (57). These subtle phenotypes may be the result of redundancy with other Mad family members or with other cell cycle regulatory proteins. In fact, an apparently compensatory increase in Mxi1 and Mad3 expression was observed in the thymi of *mad1* knockout mice (18). Therefore, as suggested for Myc family gene deletions, functional redundancy may obscure the developmental roles of *mad* genes in targeted deletion studies (15, 67). This may be less true for Mnt, whose targeted deletion

* Corresponding author. Mailing address: Division of Basic Sciences, Fred Hutchinson Cancer Research Center, 1100 Fairview Ave. N., P.O. Box 19024, Seattle, WA 98109-1024. Phone: (206) 667-4445. Fax: (206) 667-6522. E-mail: eisenman@fhcrc.org.

† Supplemental material for this article may be found at http://mcb.asm.org/.

‡ Both authors contributed equally to this work.

in mice results in craniofacial abnormalities and perinatal lethality (71). Conditional loss of *mnt* in murine breast epithelium leads to adenocarcinomas (29). Furthermore, loss of Mnt function in fibroblasts results in enhanced proliferation and upregulation of Myc target genes (29, 46). Thus, mammalian Mnt is a tumor suppressor that presumably functions to antagonize Myc activity. However, because these studies of Mnt have been carried out in settings where wild-type Mad1 to Mad4 proteins are expressed, it is difficult to sort out the extent and consequences of the overlapping functions of these proteins.

The identification of Myc and Max homologs in *Drosophila melanogaster* has greatly facilitated genetic analysis of candidate functional pathways and targets. The *D. melanogaster* homologs of Myc and Max (dMyc and dMax) heterodimerize, bind E-box sequences, activate transcription, and in the case of dMyc, recapitulate mammalian Myc functions (19, 48, 63, 72). Furthermore, both loss-of-function and gain-of-function studies with dMyc have demonstrated it to be a positive regulator of cell growth (i.e., cell mass) (31). Here we report the identification and characterization of the third member of the Max network in *D. melanogaster*, dMnt, the sole homolog of mammalian Mad and Mnt proteins. We show dMnt to be a negative regulator of cell growth that also plays a role in regulating *D. melanogaster* body size and life span.

MATERIALS AND METHODS

Two-hybrid screen and cloning of dMnt. A two-hybrid screen was initiated expressing dMax as a fusion protein with the DNA binding domain of LexA as bait. A 0- to 4-h *Drosophila melanogaster* embryonic cDNA library fused to the *trans*-activating domain of VP16 was used to screen for interacting proteins (53). Clones that were positive for β-galactosidase expression were sequenced and used to search the National Center for Biotechnology Information database (1). The two-hybrid clone was then used to probe cDNA libraries to obtain full-length cDNAs for dMnt. The dMnt cDNA was isolated from a 0- to 4-h embryonic library (10), and the dMnt ΔSID and dMnt ΔZIP splice forms were isolated from an ovary library (68).

Glutathione *S*-transferase (GST) pull-down assays. The cDNAs for dMax, dMyc, dMnt, dMnt ΔSID, and dMnt ΔZIP were cloned into pCite (Novagen, Inc.) and the proteins were expressed in a rabbit reticulocyte lysate (Promega) containing [^{35}S]methionine. dMnt bHLHZ (amino acids [aa] 149 to 386) and dMnt bHLH (aa 149 to 335) were cloned into the pGEX-5X-1 vector (Pharmacia), and fusion proteins were expressed in *Escherichia coli*. Pull-down assays were performed as previously described (28).

Antibody generation. Monoclonal antibodies (P5D6) to a GST fusion protein containing aa 149 to 248 of dMnt were generated by the Fred Hutchinson Cancer Research Center Antibody Development Facility (Seattle, WA). dMnt-GST fusion proteins were expressed in *E. coli* and purified on glutathione Sepharose beads (Pharmacia). Antibody specificity was determined by detection of in vitro-translated dMnt isoforms, but not unrelated proteins such as dMyc, in immunoblot assays and immunostaining of dMnt mutant tissues (see Fig. 3B).

Expression analysis. Immunocytochemistry was performed with dMnt-specific monoclonal antibodies or anti-ELAV (embryonic lethal abnormal visual system) antibody (47) (Developmental Studies Hybridoma Bank). Secondary antibodies used were an anti-mouse antibody conjugated to Cy3 (Zymed) and anti-rat antibody conjugated to fluorescein isothiocyanate (Jackson ImmunoResearch). DNA was stained with Hoechst 33258 (Acros). Images were captured with a Leica TCS SP confocal microscope.

Fly stocks. All flies were grown at 25°C unless otherwise indicated. w^{1118}, *en-GAL4/CyO*;UAS-*GFP*, *ey-GAL4/CyO*, *yw,hs-FLP122*, *w*;;*Actin5C>CD2>GAL4*, UAS-*GFP* (45, 52), *yw*;;[Δ*2-3*]*Sb*/*TM6B*, and *EP*(*X*)*1559* (58) (kindly provided by Gerald Rubin's lab), *dmnt*^{1} (or *dmnt*^{2})/*Binsinscy* flies were used.

UAS-mediated ectopic expression and FACS analysis. pUAS-dMnt, pUAS-dMnt ΔSID, and pUAS-dMnt ΔZIP were constructed by cloning the corresponding cDNAs into the pUAST vector (9). Standard P-element transformation was used to introduce the constructs into the *Drosophila* germ line (60). The Flp/Gal4 method (44, 52, 69) was used to generate random clones overexpressing upstream activation sequence (UAS)-regulated transgenes. Flp/Gal4 clones were induced by heat shock for 1 h at 37°C (in an air incubator) 48 h after egg deposition. Clones for fluorescence-activated cell sorting (FACS) analysis or confocal microscopy were analyzed 120 h after egg deposition. FACS analysis was performed as previously described (44). For confocal analysis, wing disks from third-instar larvae were fixed in 4% paraformaldehyde in phosphate-buffered saline for 45 min, washed, and stained with propidium iodide for nuclear staining. A Leica TCS SP confocal microscope was used.

P-element excision screen. *dmnt* mutants were generated in an imprecise P-element excision screen using a stock *EP*(*X*)*1559* (58) containing a P-element insertion between the second and third exons of dMnt. Briefly, homozygous *EP*(*X*)*1559* females were crossed with *Binsinscy*;;[Δ*2-3*]*Sb*/+ males, then *EP*(*X*)*1559*/*Binsinscy*;;[Δ*2-3*]*Sb*/+ females were crossed with *Binsinscy* males or *EP*(*X*)*1559*;;[Δ*2-3*]*Sb*/+ males were crossed with *Df*/*Binsinscy* females. Viable white-eyed male and female offspring were analyzed by PCR analysis using primer pairs consisting of a P-element-specific primer and a dMnt genomic primer flanking the left or right of the P-element insertion site. The lines which appeared to have a P-element excision event were further analyzed by PCR analysis using primers specific to individual exons and a primer set that amplifies the closest exon of the neighboring gene, *ral A*. The regions of deletion for the two mutant lines were also mapped by Southern blotting (data not shown).

RT-PCR analysis. Reverse transcription-PCR (RT-PCR) analysis was performed to detect the presence of dMnt, dMnt ΔSID, and dMnt ΔZIP mRNA. Total RNA from adult males was isolated with TRIzol (Invitrogen) according to the manufacturer's instructions. Sensiscript reverse transcriptase (QIAGEN) was used in the RT reaction according to the manufacturer. dMnt and dMnt ΔZIP cDNAs (detection was based on size differences of the PCR products) were then PCR amplified (one cycle of 94°C for 3 min; 35 cycles of 94°C for 1 min, 56°C for 1 min, and 72°C for 1 min 30 s; one cycle of 72°C 7 min) with a 5′ primer (5′-GGTGCTCCTCGAGGCGGCTC-3′) and a 3′ primer (5′-CGGGTGCCCG CGCCATTAC-3′), primers 1 and 3, respectively (see Fig. 5A). The dMnt ΔSID cDNA was PCR amplified using the same conditions mentioned above with a 5′ primer (5′-TCGGAGGACGATAATTCCTC-3′) and the same 3′ primer mentioned above, primers 2 and 3, respectively (see Fig. 5A). Rp49 was used as the loading control. PCR products were run on a 1.5% agarose gel containing ethidium bromide.

Growth analysis. *dmnt*^{1} and *dmnt*^{2} mutant adult males were used to measure the average fly weight and cell size in the adult wing. Fifty first-instar larvae from a 6-h collection were seeded in a vial and left until 3 days after eclosion when the males were collected, snap-frozen on dry ice, and stored at −70°C. Eight vials of each genotype were collected, and the average adult male weight was calculated for each genotype. Cell size studies were performed using the wings from these adult males. Twelve wings (six individuals) from each genotype were dissected and mounted (Canada Balsam; methyl salicylate). Bright-field microscopic images were captured using a Leitz DMRD microscope and a RT Slider Spot digital camera (Diagnostic Instruments, Inc.). The number of bristles recorded in a defined unit area was determined and averaged for each genotype. Both the weight and cell size studies were repeated three times with separate parents.

Longevity assays. *dmnt*^{1}, *dmnt*^{2}, and P-element precise excision allele (wild-type control) virgins were collected and allowed to age in the absence of males at a density of 20 flies per vial. Flies were transferred to fresh food every 3 days, and scores for dead flies were determined at this time. Longevity studies were repeated three times with independent sets of parents. The average percent survivorship from the three independent experiments was then calculated for each collection point.

RESULTS

Identification of dMnt. Following the identification of the *D. melanogaster* homologs of Myc and Max, we initiated a two-hybrid screen to identify other dMax-interacting proteins. Full-length dMax fused to the LexA DNA binding domain was used as bait to screen a *D. melanogaster* 0- to 4-h embryonic cDNA-VP16 fusion library. Several overlapping interacting clones contained significant homology to the bHLHZ domain of mammalian Mnt and Mad proteins. Full-length cDNAs were then isolated from 0- to 4-h *D. melanogaster* embryonic and

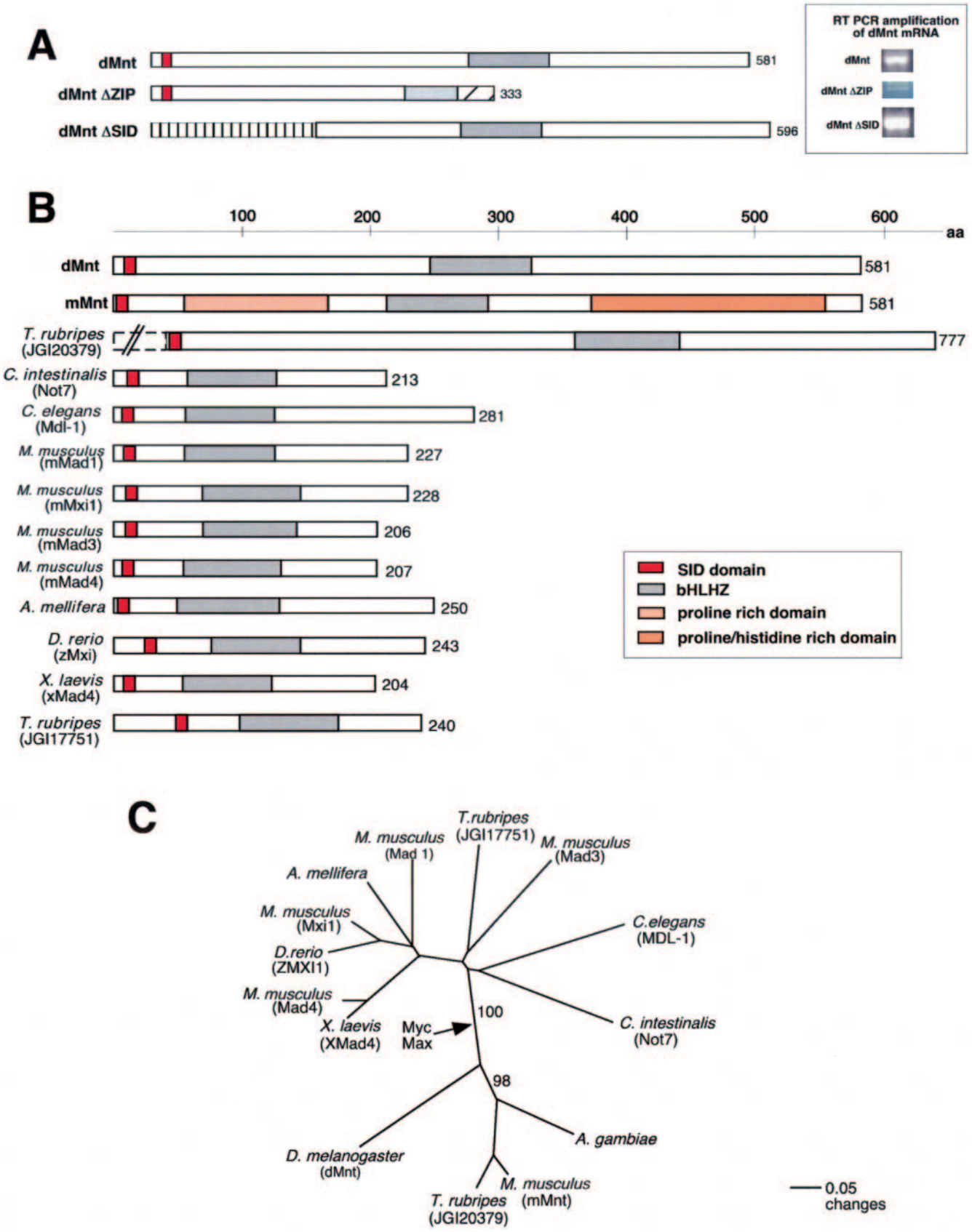

FIG. 1. dMnt is the sole *Drosophila* homolog of mammalian Mnt and Mad family members. (A) Schematic diagram of the protein structure of dMnt splice forms dMnt, dMnt ΔZIP, and dMnt ΔSID. dMnt contains the Sin-interacting domain (SID) and bHLHZ domains, the hallmark

ovary cDNA libraries. Three splice variants were isolated from these libraries (Fig. 1A). One form, which we will refer to as dMnt, contains the two conserved domains that are characteristic of Mnt and Mad family members: SID, required for interaction with the corepressor Sin3, and the bHLHZ domain, necessary for DNA binding and heterodimerization with Max (for a review, see reference 39). dMnt ΔZIP contains SID and the basic helix-loop-helix domains but lacks the zipper domain. Lastly, dMnt ΔSID has a novel amino terminus lacking SID but retains the bHLHZ domain. Sequence comparisons indicate that the predicted protein sequence of SID for dMnt is 56% identical to the SID domains of mouse Mad1 and Mnt, and the bHLHZ domain is 55% and 33% identical to the bHLHZ domains of mouse Mnt and Mad1, respectively. RT-PCR analysis indicates that all three forms are expressed in adult male flies (Fig. 1A).

Although dMnt possesses the two functionally conserved domains common to Mnt and Mad family members, it lacks the proline-rich and proline/histidine-rich domains characteristic of Mnt. To more precisely classify this newly identified *D. melanogaster* gene, we examined its phylogeny more closely. Figure 1B illustrates the similarities and differences between Mnt and Mad proteins and the positions of functionally conserved domains in various organisms. dMnt (581 aa) is similar in size to mammalian Mnt (581 aa) and the predicted fugu Mnt (*Takifugu rubripes*, JGI20379; 777 aa) compared to Mad proteins (~250 aa). Also, the overall organization of dMnt is more similar to that of mammalian Mnt. The SID and bHLHZ domains of Mnt proteins are approximately 200 aa apart, whereas the Mad proteins have an average of 30 aa that separate these two domains. To determine relatedness among *mnt* and *mad* genes in various organisms, we constructed a phylogenetic tree based on sequence homology within the bHLHZ domain (81 aa) (Fig. 1C). This domain contained the largest block of amino acids common to all Max network proteins analyzed. The tree indicates that the dMnt bHLHZ and the predicted bHLHZ regions for the *Anopheles gambiae* mosquito and *T. rubripes* are more closely related to mammalian Mnt than to other members of the Mad family of proteins. These analyses indicate that the gene products we identified are overall more homologous to Mnt. A search of the *D. melanogaster* genome sequence has failed to identify any other Mad-related protein. Thus, dMnt and its splice forms may be considered to be the sole *D. melanogaster* homolog of both Mnt and Mad.

dMnt is biochemically and functionally similar to vertebrate Mad and Mnt proteins. Vertebrate Myc, Max, and Mad/Mnt are all members of the bHLHZ class of transcription factors in which the bHLHZ domains mediate highly specific heterodimerization of Myc and Mad with Max as well as sequence-specific DNA binding (3, 6). To determine whether dMnt heterodimerizes with dMax, we carried out in vitro binding assays. Chimeric proteins in which GST was fused to the dMnt bHLHZ domain or the dMnt ΔZIP bHLH domain were bacterially expressed and purified. GST alone or GST fusion proteins were incubated with in vitro-transcribed and in vitro-translated [^{35}S]methionine-labeled dMax, dMyc, or each of the three dMnt splice forms (Fig. 2A). GST alone did not specifically associate with any of the in vitro-translated proteins. However, the GST-dMnt bHLHZ fusion protein interacted specifically with dMax but did not interact with dMyc or any of the dMnt splice forms. The GST-dMnt ΔZIP bHLH fusion protein failed to interact with dMax, dMyc, or any of the dMnt splice forms. These results demonstrate that dMnt is able to heterodimerize with dMax through the bHLHZ domain but is unable to homodimerize or interact with dMyc. In addition, the leucine zipper domain is required for dMnt heterodimerization with dMax.

Mammalian Mad family members and Mnt contain an amino-terminal SID that is required for transcriptional repression (4, 61). The SID domains of Mad proteins have been previously demonstrated to interact with the second paired amphipathic helix (PAH2) domain of the Sin3 corepressor (4, 11, 61). Because dMnt possesses a region similar to mammalian SIDs, we performed GST pull-down experiments to determine whether dMnt associates with the PAH2 domain of dSin3. GST or GST-dSin3 (PAH2) fusion protein was incubated with labeled, in vitro-transcribed, and in vitro-translated dMnt splice forms (Fig. 2B). GST-dSin3(PAH2) interacted specifically with the two dMnt splice forms containing SID but did not bind the dMnt ΔSID form. No interaction of the dMnt splice forms with GST alone was observed.

Vertebrate Myc-Max and Mad-Max heterodimers have been demonstrated to bind specifically to the consensus E-box sequence CACGTG (4, 6, 61), and *D. melanogaster* Myc-Max dimers bind the same E-box sequence (19, 63). We tested in vitro-translated dMnt, dMnt ΔZIP, or dMnt ΔSID together with dMax in electrophoretic mobility shift assays and determined that dMnt-dMax and dMnt ΔSID-dMax heterodimers bind specifically to a labeled CACGTG oligonucleotide (see Fig. S1 in the supplemental material). As expected, given that dMnt ΔZIP is unable to heterodimerize with dMax (Fig. 2A), no specific binding to the labeled oligonucleotide was observed in the sample containing dMnt ΔZIP and dMax.

The DNA binding activity of these proteins is related to their transcriptional function. Synthetic reporter genes, as well as cellular target genes, are transcriptionally activated by both

of all Mnt and Mad family proteins. The dMnt ΔZIP form lacks the zipper domain (due to a splicing event that omits the exon containing the zipper domain) and contains a unique COOH terminus (due to a reading frameshift; marked by the region with short vertical lines). The dMnt ΔSID form contains a unique NH terminus (marked by the hatch marks) that lacks the SID domain. See Fig. 5A for gene structure and splicing map. RT-PCR analyses indicate that all three splice forms are expressed in adult males. Primer locations are indicated in Fig. 5A. (B) Schematic diagram of the protein organization of dMnt and homology to Mnt and Mad proteins from various organisms. Mnt and Mad proteins from *Takifugu rubripes*, *Ciona intestinalis*, *Caenorhabditis elegans*, *Mus musculus*, *Apis mellifera*, *Danio rerio*, and *Xenopus laevis* are shown. This diagram illustrates similarities in the protein organization of dMnt, mMnt, and a putative Mnt protein in *Takifugu rubripes* and the differences between dMnt and Mad proteins. The bHLHZ domain of dMnt was used in a BLAST search (National Center for Biotechnology Information [1]) to identify proteins with homology in this domain. (C) A phylogenetic tree based on sequence homology within the bHLHZ domain (81 aa) was generated to determine relatedness among Mnt and Mad genes in various organisms (including *Anopheles gambiae*). The tree was generated using the programs CLUSTAL_X (70a) and PAUP 4.0 (Sinauer Associates, Inc., Sunderland, MA).

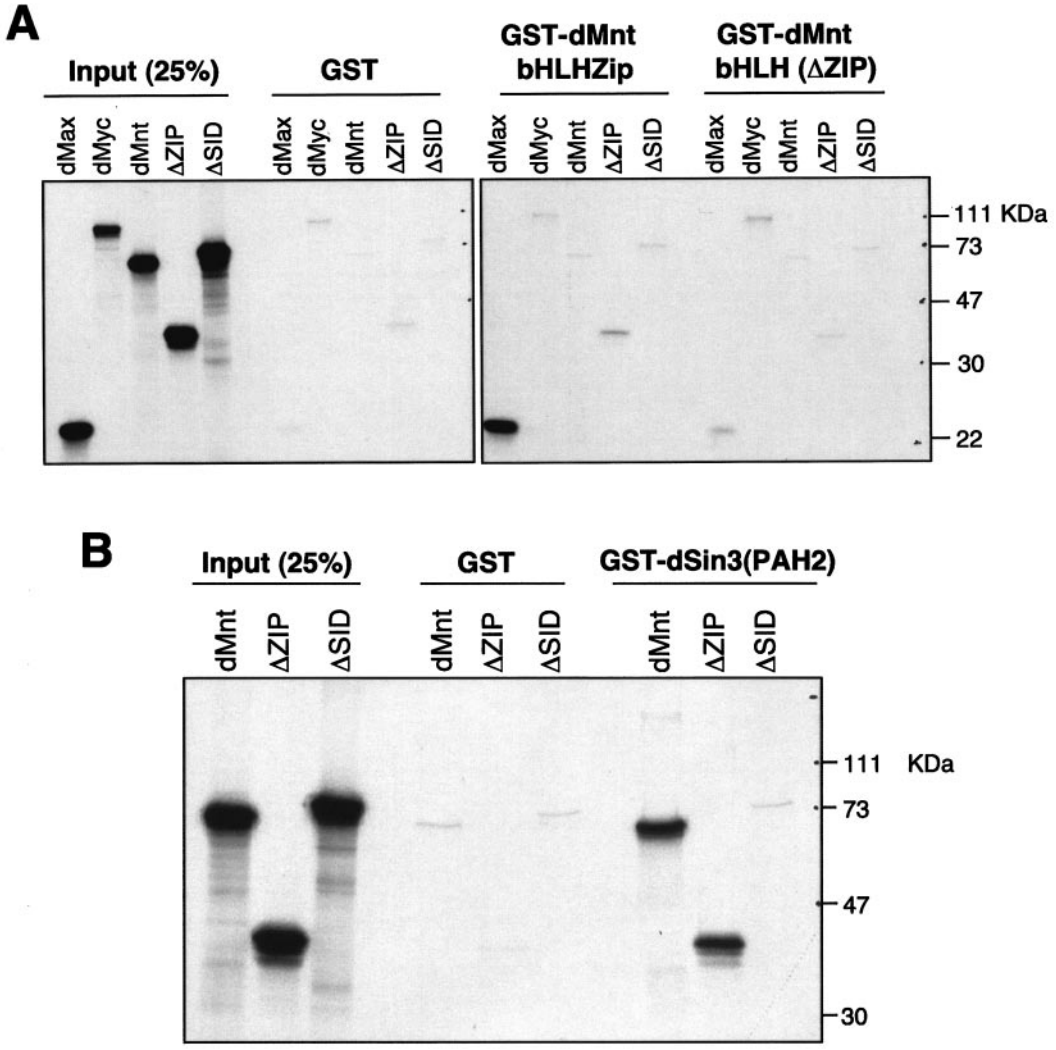

FIG. 2. dMnt interacts with dMax and dSin3. (A) In vitro-translated, ^{35}[S]methionine-labeled dMax, dMyc, dMnt, dMnt ΔZIP, and dMnt ΔSID proteins were mixed with GST, GST–dMnt-bHLHZip, or GST–dMnt-bHLH (lacking the ZIP domain) in a GST pull-down assay. (B) In vitro-translated, ^{35}[S]methionine-labeled dMnt proteins were mixed with GST or a GST-fusion protein containing the paired amphipathic helix domain 2 (PAH2) of dSin3. This domain interacts specifically with the SID domain of Mnt and Mad proteins. The GST proteins and bound, in vitro-translated products were isolated with glutathione Sepharose beads and analyzed on a 10% sodium dodecyl sulfate-polyacrylamide gel.

vertebrate and *D. melanogaster* Myc-Max heterodimers and are transcriptionally repressed by mammalian Mad-Max and Mnt-Max. Activation and repression by these groups of heterodimers are dependent on the presence of the E-box sequence (for reviews, see references 21, 37, 49, and 77). We found that expression of dMnt and dMax repressed transcription of a reporter construct containing an E-box (CAC GTG) twofold compared to empty vector control (see Fig. S2 in the supplemental material). In contrast, the dMnt ΔSID and dMnt ΔZIP splice forms failed to influence transcriptional activity relative to empty vector. Taken together, these results indicate that dMnt, like vertebrate Mad and Mnt proteins, dimerizes with dMax, binds E-box sequences, and represses transcription of an E-box-containing promoter in a SID-dependent manner.

Expression of dMnt during development. Expression of mammalian Mad proteins is generally associated with differentiation and organogenesis, while Mnt appears to be more constitutively expressed in both actively dividing cells and those that are exiting the cell cycle (26, 27, 42, 56). To examine the expression pattern of dMnt, we raised a monoclonal antibody, P5D6, to the region common to all three dMnt splice forms (see Materials and Methods for details). To verify the specificity of the dMnt antibody, the larvae of a *dmnt* null mutant (*dmnt*^{1}) and a mutant that retains the dMnt ΔSID transcript (*dmnt*^{2}) were stained with P5D6 (see below for derivation and analysis of mutants). As seen in Fig. 3Ba to c, nuclear staining is clearly seen in wild-type cells and, to a lesser degree in *dmnt*^{2} mutant cells, but is not detectable in *dmnt*^{1} mutant cells in larval salivary gland cells. These results support the observation that P5D6 is a dMnt-specific antibody.

Although *dmnt* mRNA is maternally deposited and is present until cellularization (data not shown), dMnt protein is first detected in cells of the epidermis at embryonic cell cycle

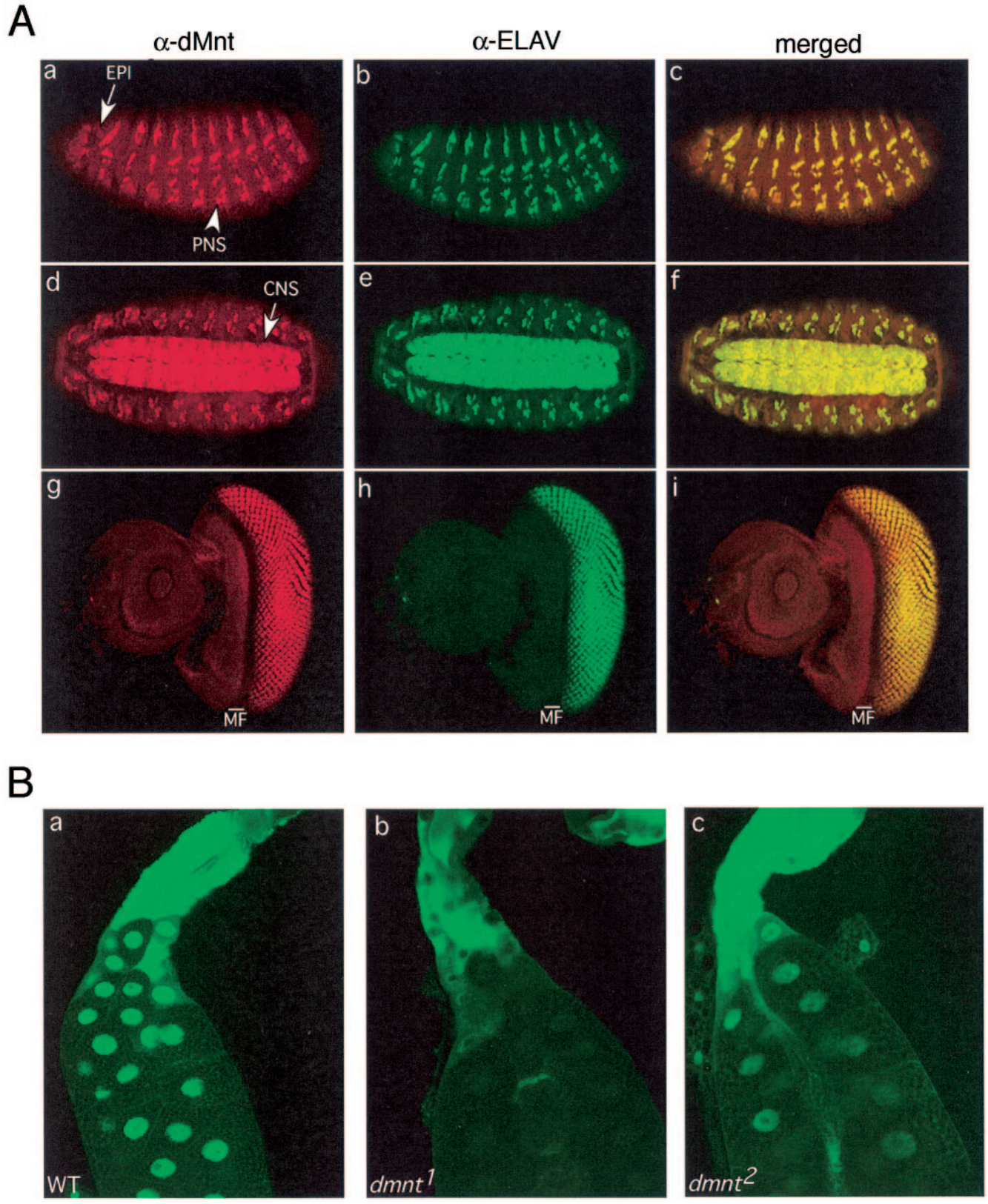

FIG. 3. Endogenous expression of dMnt. (A) A monoclonal antibody recognizing all three dMnt splice forms was used in immunofluorescence assays to detect endogenously expressed dMnt splice forms. dMnt protein is detectable in the cells of the epidermis (EPI) (a), the central nervous system (CNS) (d) and peripheral nervous system (PNS) (a) of late-stage embryos, and the peripheral nervous system cells in eye-antennal disks of third-instar larvae (g) posterior to the morphogenetic furrow (MF). Antibodies to the neural antigen ELAV (α-ELAV) identify differentiated cells of the central and peripheral nervous systems (b, e, and h). α-dMnt, anti-dMnt antibody. (B) The specificity of the monoclonal antibody to dMnt proteins is demonstrated by the nuclear staining of salivary glands from wild-type (WT) third-instar larvae and the absence of specific nuclear staining in a dMnt null mutant (*dmnt*^{1}) and to a lesser degree in a dMnt hypomorph (*dmnt*^{2}).

17 (stage 11), coincident with these cells ceasing proliferation and beginning differentiation (Fig. 3A). At this and subsequent stages, dMnt is also expressed in peripheral and central nervous system cells, as evidenced by the colocalization of dMnt and the neural antigen ELAV (47) (Fig. 3Aa to f). dMnt expression is not, however, limited to cells that are differentiating during embryogenesis; dMnt is also expressed in the embryonic salivary gland primordium at stage 11 when these cells are actively endocycling (data not shown).

dMnt is also expressed in both differentiating and actively dividing cells during the third larval instar of *D. melanogaster* development. During eye imaginal disk development, cells are recruited to become peripheral nervous system cells and express the neural antigen ELAV posterior to a morphological marker called the morphogenetic furrow (MF). dMnt is predominantly expressed in differentiated cells posterior to the MF. However, a group of dMnt-positive, ELAV-negative cells is detectable at the MF, indicating that dMnt is expressed as the neural fate of these cells is being determined (Fig. 3Ag to i). In addition, dMnt is expressed in actively dividing peripodial membrane cells of the wing and eye-antennal imaginal disks in third-instar larvae (K. McClure, personal communication; also data not shown). dMnt is also present in endocycling salivary gland (51) and fat body cells (Fig. 3B; data not shown). dMnt is therefore expressed in a temporally and spatially dynamic pattern in both actively replicating mitotic and endoreplicating tissue and differentiating cells.

Ectopic expression of dMnt inhibits cellular growth and proliferation. To determine whether expression of dMnt splice variants can influence cell behavior in *D. melanogaster*, we used the UAS/GAL4 expression system (9) to express dMnt in endocycling and mitotically dividing cells during development. dMnt proteins were ectopically expressed in the developing eye (employing an *eyeless*-GAL4 driver) and posterior compartments (*engrailed*-GAL4). In all tissues ectopically expressing the dMnt cDNA, we observed a marked reduction in the size of the respective adult structure (see Fig. S3 in the supplemental material). These phenotypic changes were more severe when dMnt and dMax were ectopically coexpressed in these tissues, suggesting that the observed dMnt effects were mediated by the transcriptional repression activity of dMnt-dMax heterodimers. We did not observe any obvious adult phenotypes when dMax, dMnt ΔSID, or dMnt ΔZIP was expressed using these drivers (see Fig. S3A in the supplemental material; also data not shown).

We measured proliferation in cell clones ectopically expressing the dMnt cDNA to determine whether the observed dMnt ectopic expression phenotypes were the result of dMnt's ability to inhibit proliferation utilizing the Flp/Gal4 method (see Materials and Methods for details). We compared the sizes of clones ectopically expressing dMnt with GFP to clones expressing GFP alone in both the imaginal wing disk (Fig. 4A) and the fat body (51). Clones ectopically expressing dMnt were significantly smaller than clones expressing GFP alone. To determine whether the reduced clone size was due to an inhibition of proliferation and/or growth or apoptosis, dMnt was coexpressed with the baculovirus apoptosis inhibitor p35. There was no significant change in the size of clones coexpressing dMnt and p35 compared to clones expressing dMnt without p35 (data not shown). These results support the observation that dMnt expression is associated with an inhibition of cellular proliferation. Surprisingly, in contrast to what was observed with the eyeless-GAL4 and engrailed-GAL4 drivers, expression of the dMnt ΔSID or dMnt ΔZIP splice form in the wing disks of random clones appeared to have an intermediate effect on proliferation relative to dMnt (Fig. 4A). Because only the latter experiments were carried out under conditions where cell competition is known to occur, it is likely that even relatively weak effects of dMnt ΔSID or dMnt ΔZIP compared to dMnt would be detected. To determine whether the smaller clone size caused by dMnt expression was due to effects on cell cycle or cell size, we dissociated wing disk cells and examined them using flow cytometry (Fig. 4B). We compared GFP-positive cells, which express the transgene, to GFP-negative cells, which represent the wild-type cell profile. When dMnt was expressed, we observed an increase in the population of cells in the G_0/G_1 phase of the cell cycle and a decrease in the population of cells in S and G_2/M. When we compared the relative sizes of the cells ectopically expressing dMnt and the nonexpressing population by forward scatter (Fig. 4B), we found that dMnt-expressing cells were significantly smaller than the wild-type cells. This size difference is not due to the increased fraction of G_0/G_1 cells in the dMnt-expressing population because when we gated and compared individual cell cycle phases, we found that the size difference was observed in all phases (data not shown). Expression of the dMnt ΔSID or dMnt ΔZIP proteins resulted in no detectable effects on cell cycle phasing or cell size, suggesting that these splice forms are likely to act through a mechanism distinct from that of dMnt. Overall, these results indicate that expression of dMnt has effects on cellular proliferation, cell cycle progression, and cell growth.

Isolation of *dmnt* mutant alleles. To analyze the effects of loss of *dmnt* function, we searched the *D. melanogaster* database for any mutations in the *dmnt* genomic region (cytological region 3E5). We identified two P-element insertions in the *dmnt* gene and one insertion immediately upstream of the putative transcription start site. We then initiated an imprecise P-element excision screen to obtain stronger *dmnt* mutant alleles. By mobilizing the P-element [*EP(X)1559*] (58), we generated two independent *dmnt* mutant alleles, $dmnt^1$ and $dmnt^2$, and a precise excision which serves as a wild-type control allele (Fig. 5A). On the basis of genomic PCR and Southern blotting analysis, $dmnt^1$ is a null allele. All exons contributing to the open reading frame of dMnt are deleted in this allele. $dmnt^2$ contains a smaller deletion that removes the exon containing the translational start codons of the dMnt and dMnt ΔZIP splice forms but does not extend to the exon containing the translational start codon of the dMnt ΔSID splice form. RT-PCR analysis demonstrated that $dmnt^1$ lacks mRNA for the dMnt, dMnt ΔZIP, and dMnt ΔSID splice forms (Fig. 5B), while $dmnt^2$ lacks detectable mRNA for the dMnt and dMnt ΔZIP splice forms but retains the mRNA for dMnt ΔSID (Fig. 5A and B). In addition, we performed RT-PCR analyses on the neighboring gene, *ralA*, to determine whether expression of this gene was affected in the *dmnt* mutant alleles. No difference in *ralA* mRNA expression was detectable for either of the *dmnt* mutant alleles compared to the wild-type control, indicating that our deletion has not extended beyond the *dmnt* locus (data not shown).

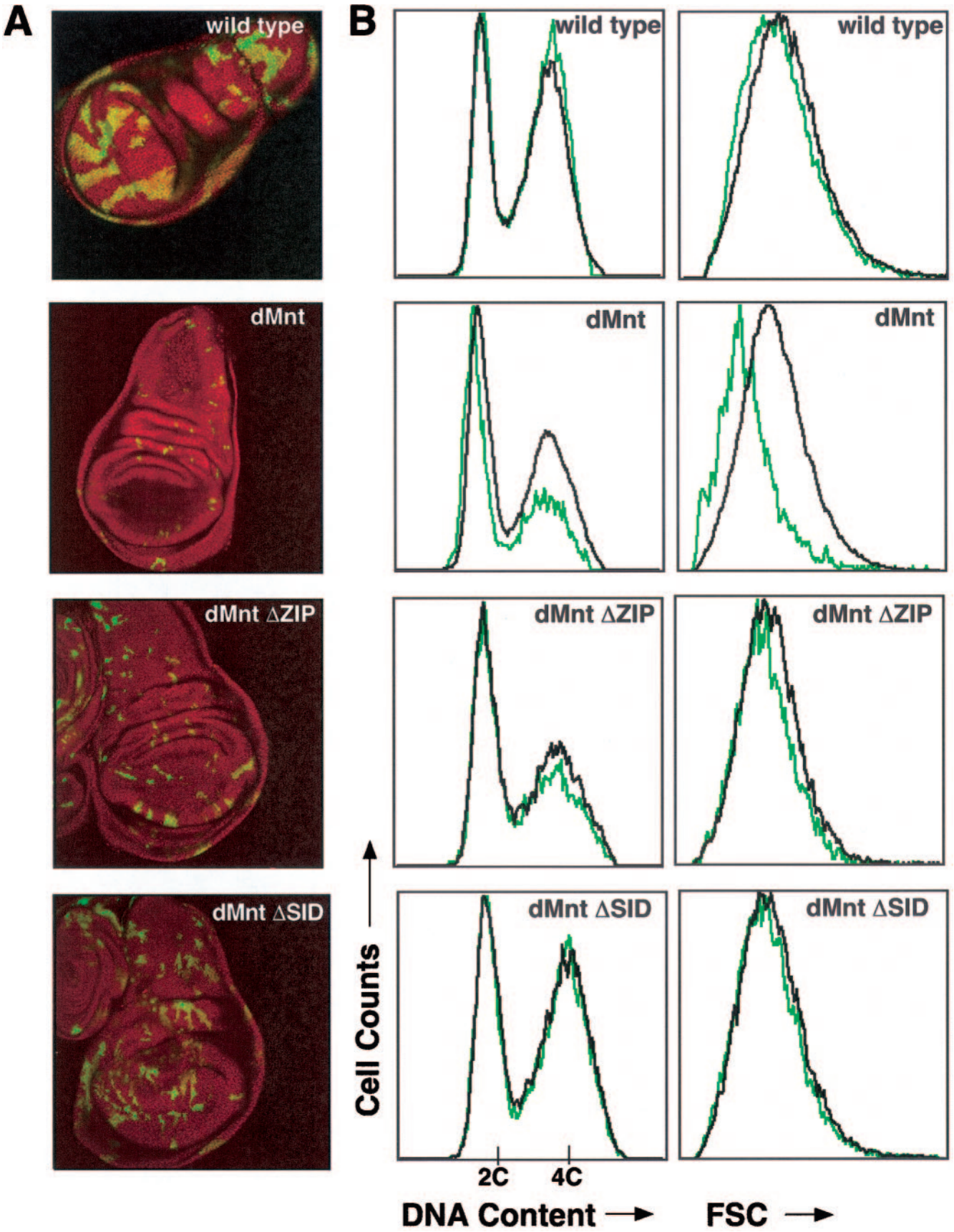

FIG. 4. Expression of dMnt splice forms is associated with inhibition of proliferation and growth. (A) Random clones ectopically expressing GFP alone (wild type) or GFP and dMnt, dMnt ΔZIP, or dMnt ΔSID transgene in third-instar wing disks (see Materials and Methods). (B) Dissociated cells from random clones in third-instar wing disks (as in panel A) were analyzed by FACS analysis of GFP-positive and GFP-negative cells. Cell cycle phasing (left columns) and cell size (forward scatter [FSC], right columns) were plotted for wild-type, GFP-negative (black trace), and transgene-expressing, GFP-positive (green trace) cells.

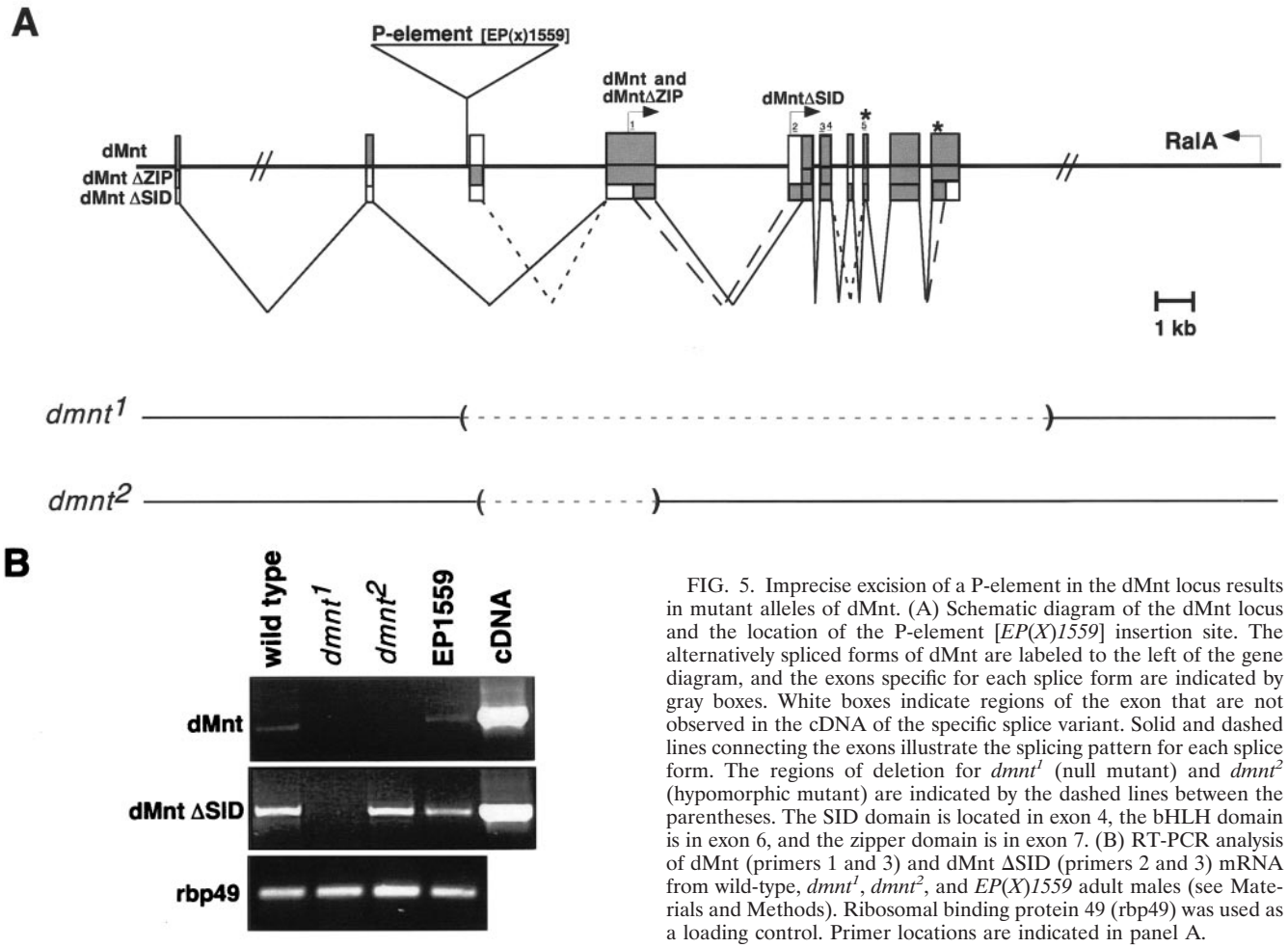

FIG. 5. Imprecise excision of a P-element in the dMnt locus results in mutant alleles of dMnt. (A) Schematic diagram of the dMnt locus and the location of the P-element [*EP(X)1559*] insertion site. The alternatively spliced forms of dMnt are labeled to the left of the gene diagram, and the exons specific for each splice form are indicated by gray boxes. White boxes indicate regions of the exon that are not observed in the cDNA of the specific splice variant. Solid and dashed lines connecting the exons illustrate the splicing pattern for each splice form. The regions of deletion for *dmnt*^{1} (null mutant) and *dmnt*^{2} (hypomorphic mutant) are indicated by the dashed lines between the parentheses. The SID domain is located in exon 4, the bHLH domain is in exon 6, and the zipper domain is in exon 7. (B) RT-PCR analysis of dMnt (primers 1 and 3) and dMnt ΔSID (primers 2 and 3) mRNA from wild-type, *dmnt*^{1}, *dmnt*^{2}, and *EP(X)1559* adult males (see Materials and Methods). Ribosomal binding protein 49 (rbp49) was used as a loading control. Primer locations are indicated in panel A.

dmnt^1 and *dmnt*^{2} mutants are homozygous viable and fertile with no detectable decrease in fitness. To determine whether there are any delays or developmental defects during embryogenesis, we tested hatching rates on the two homozygous mutant lines and compared them to a wild-type (precise excision) control and the parental *EP(X)1559* allele. We observed no significant differences in the hatching percentage or rate in the mutants compared to the wild-type control, suggesting that the loss of dMnt has no significant effects on developmental timing during embryogenesis. We also analyzed larval development and did not detect any delays in larval molting, pupation, or eclosion. These results suggest that dMnt is not essential for the normal developmental program.

dMnt mutants have a growth phenotype and are short-lived. Because ectopic expression of dMnt inhibits cellular proliferation and growth, we determined whether loss of dMnt function influences weight and cell size in adult flies. We compared the average individual weights of *dmnt* mutant adult males and wild-type control males and observed that both *dmnt*^{1} and *dmnt*^{2} mutant males are 20% and 12% heavier than wild-type controls (Fig. 6A). Cell size was measured by determining trichome density (each trichome represents one cell) in a defined area of the adult wing. *dmnt*^{1} mutant males had 18% fewer cells in a unit area and *dmnt*^{2} mutants had 10% fewer cells than the wild-type controls (Fig. 6B), indicative of increased cell size. These results demonstrate that dMnt proteins normally play a role in limiting cellular growth.

Several mutants that affect adult body size, such as those that compromise insulin signaling in *D. melanogaster*, also influence life span (14, 70). To test whether dMnt mutant adults have an altered life expectancy, *dmnt*^{1} and *dmnt*^{2} virgins were collected, their ages were determined, and the number of dead flies was scored every 3 days and compared to the death rate of virgins from isogenic wild-type controls. The results are the average of three independent and highly reproducible experiments. The average life spans of *dmnt*^{1} and *dmnt*^{2} females were 41 and 48 days, respectively, compared with 54 days for wild-type controls (Fig. 7). This reduction of 13 days represents a significant decrease (24%) in the life span of the fly. The maximal life expectancy (90% mortality) is also reduced in *dMnt* mutant animals, with wild-type flies living an average of 71 days compared with 59 and 63 days for *dmnt*^{1} and *dmnt*^{2} alleles, respectively (Fig. 7). The intermediate phenotype observed for *dmnt*^{2} in life span is consistent with its less severe effect on adult cell and body size, suggesting that *dmnt*^{2} is likely to be a hypomor-

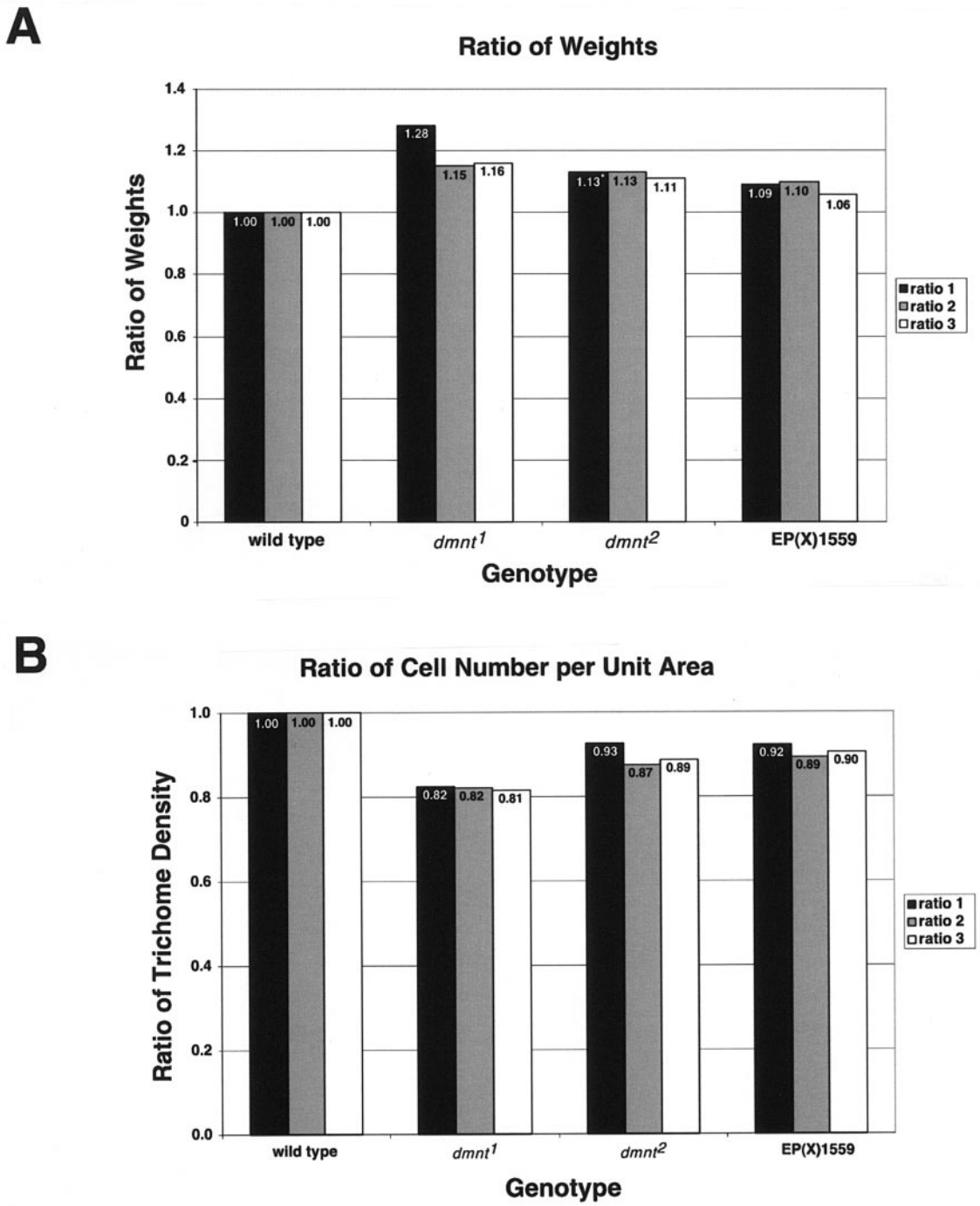

FIG. 6. Expression of dMnt splice variants is required for normal growth. (A) *dmnt*^{1} and *dmnt*^{2} mutant males were used to analyze dMnt's role in normal growth control of the fly. The ratio of *dmnt* mutant/wild-type control (precise excision) was calculated on the basis of the average weight of an individual adult male fly for three independent experiments (black, gray, and white bars). (B) Growth was also measured by cell size in the adult male wing. Cell size was determined by enumerating the number of trichomes (one trichome/cell) in a unit area in a designated region of the wing. The ratio of trichome density was calculated as the average number of cells in one unit area of *dmnt* mutant/wild type for three independent experiments (black, gray, and white bars). The precise excision of the *EP(X)1559* allele was used as the wild-type control. The *P* values were determined by Student's *t* test. All *P* values were <0.01, with the exception of the ratio with the white asterisk, which had a *P* value of <0.02.

phic allele. While *dmnt* mutant females have a shorter life span than an isogenic wild-type control, these flies are generally not unhealthy. *dmnt* mutant strains can be kept as homozygous stocks and show no developmental delays. Furthermore, *dmnt* mutant larvae and adults are neither more sensitive to starvation (see Fig. S4 in the supplemental material) nor more susceptible to bacterial infection (data not shown). Therefore, it is unlikely that the shortened life span of the mutants is due to

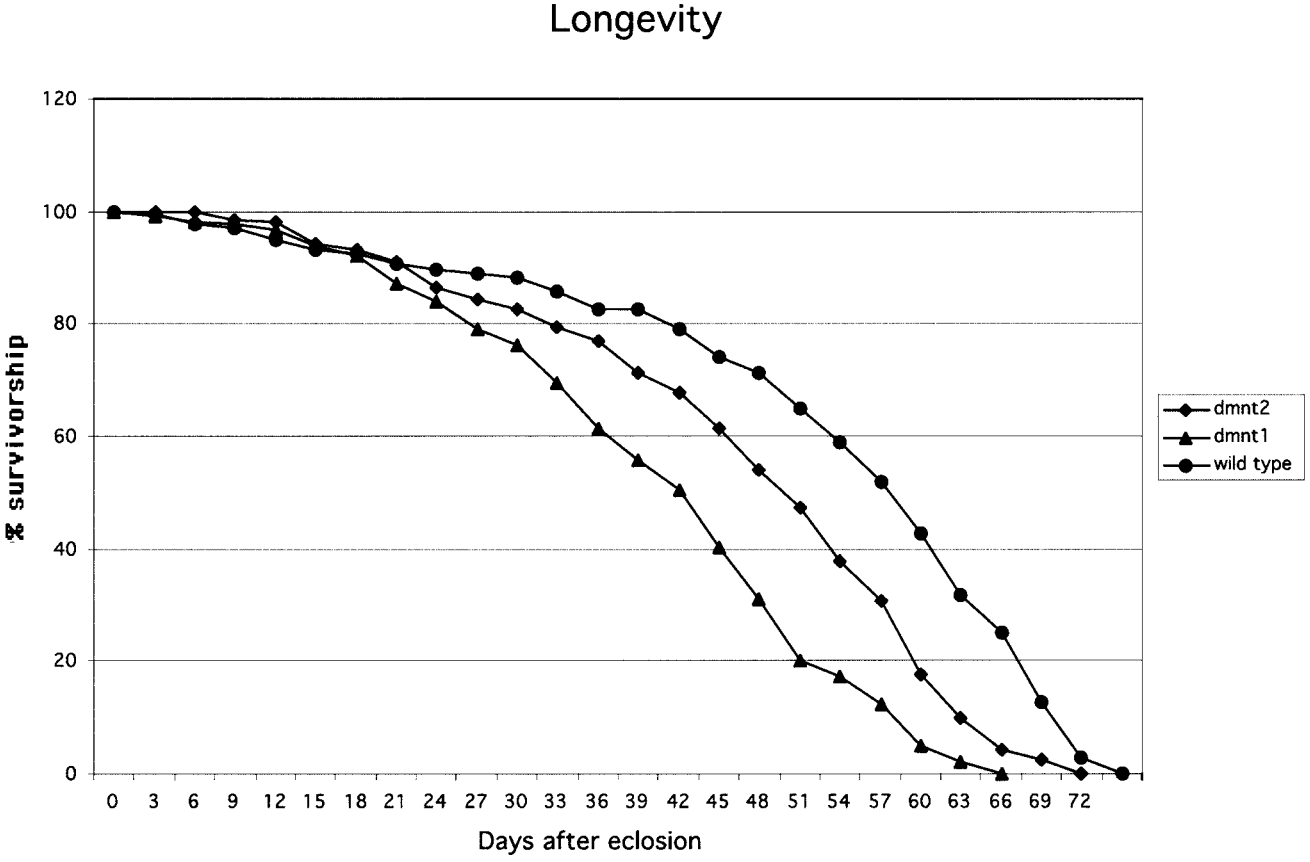

FIG. 7. Expression of dMnt splice forms affects the life span of the fly. *dmnt*^{1} and *dmnt*^{2} mutants were used to analyze dMnt's role in life span. Virgin females were collected, their ages were determined, and the number of dead flies was scored every 3 days (see Materials and Methods). The average percent survivorship from three independent experiments was plotted for each collection point. The average decrease in survivorship with respect to the isogenic control for the wild type and *dmnt*^{1} mutants or the wild type and *dmnt*^{2} mutants was 24% ± 5% and 11% ± 6%, respectively.

developmental defects, infection, or generalized unhealthiness. Taken together, these results suggest that dMnt plays a role in regulating life span (see Discussion).

DISCUSSION

The identification and characterization of dMnt reported here, considered together with earlier studies on dMyc and dMax (8, 19, 31, 63), demonstrate that the components of the vertebrate "Max network," their major protein-protein interactions, and their antagonistic transcriptional functions are conserved in *D. melanogaster*.

dmnt is the sole homolog of *mnt* and *mad* genes in *D. melanogaster*. Sequence comparison and phylogenetic tree construction based on the bHLHZ domain indicate that the protein product of this gene is most similar to vertebrate Mnt (Fig. 1). In addition to the bHLHZ domain, dMnt possesses the SID domain characteristic of mammalian Mnt and the four Mad family proteins. We show that both these domains are functional—the dMnt bHLHZ mediates association with Max and DNA binding, while the dMnt SID interacts directly with the Sin3 corepressor (Fig. 2). On the other hand, dMnt lacks the proline-rich and proline/histidine-rich domains characteristic of mammalian Mnt. Because at this time there is no data indicating that these domains are required for Mnt function, their absence in *D. melanogaster* Mnt cannot be taken as evidence of functional divergence. We surmise that dMnt represents a progenitor of the vertebrate Mad family and Mnt proteins. This notion is consistent with the developmental patterns of expression we have observed for dMnt (Fig. 3A) which appear similar to those for mammalian Mad proteins (expressed during cell cycle exit) as well as Mnt (expressed in proliferating cells). The numerous vertebrate paralogs are likely a reflection of the more complex and diverse regulation imposed on these genes during vertebrate development.

It is probably not a coincidence that the alternatively spliced forms of dMnt that we have observed involve functionally significant alterations in the SID and bHLHZ domains (Fig. 1A, 2, and 5A). In contrast to dMnt, which functions as a transcriptional repressor, neither the dMnt ΔZip protein nor the dMnt ΔSID protein displayed positive or negative transcriptional activity on a synthetic reporter gene containing E-box binding sites (see Fig. S2 in the supplemental material). These forms could potentially act as dMnt dominant interfering proteins. However, both the dMnt ΔZip and dMnt ΔSID forms contain unique sequences introduced by alternative splicing and not found in dMnt (Fig. 1A and 5A). We speculate

that it is the polypeptide regions that are unique to the ΔZip and ΔSID isoforms that confer distinct E-box- and Sin3-independent functions on these proteins. For example, overexpression of dMnt, but not dMnt ΔZip or dMnt ΔSID, had strong effects on wing and eye formation (see Fig. S3 in the supplemental material). However, while all three isoforms reduced the size of random clones in the wing disk, dMnt had the most dramatic effects and also influenced cell size and cell cycle phasing (see below). By contrast, the ΔZip and ΔSID isoforms had no detectable effects on cell size or cell cycle (Fig. 4). It will be of interest to further explore potential protein interactions mediated by the alternatively spliced sequences in the ΔZip and ΔSID isoforms and to delineate in greater detail their expression patterns and biological roles.

Our imprecise excision screen of an existing allele containing a P-element insertion in the *dmnt* gene generated *dmnt*^{1}, a null allele, and *dmnt*^{2}, an allele that expresses only the dMnt ΔSID form (Fig. 5). To our surprise, both mutant alleles are viable with no obvious pattern of defects or effects on male or female fertility. We did, however, observe that *dmnt*^{1} and *dmnt*^{2} mutants were 20% and 12% heavier than their wild-type controls, respectively. Furthermore, *dmnt*^{1} and *dmnt*^{2} alleles had an average of 18% and 10% fewer cells per unit area, respectively, than the wild-type controls, indicative of increased cell size (Fig. 6). The intermediate effect observed with *dmnt*^{2}, which expresses only dMnt ΔSID, again suggests that this alternatively spliced form functions in a pathway related to the dMnt pathway. The augmentation of cell and organismal size in the dMnt mutant flies is generally consistent with dMnt acting as an antagonist of dMyc. Flies with dMyc loss-of-function alleles are smaller and have increased trichome density (19, 31, 63), while dMyc overexpression generates larger cells and flies (16, 31). Mice with single deletions of murine *mad* family genes *mad1*, *mxi1*, and *mad3* were viable, although hyperplasia, sensitivity to radiation damage, and a delay in differentiation were observed. The relatively mild phenotypes were generally ascribed to redundancy between *mad* family members. Our data derived from the *dmnt* null mutant suggest that *mad* genes are not essential for survival. However, a strong synthetic effect in mice bearing both *mad1* and *p27*^{KIP1} null alleles indicates that *mad* genes may be redundant with other genes that act to limit cell growth and proliferation (38). Interestingly, we did not observe any obvious genetic interaction or developmental or adult phenotypes in mutant flies which were hemizygous for *dmnt*^{1} and heterozygous for *dacapo*, the sole *Drosophila* p21^{CIP1}/p27^{KIP1} ortholog (data not shown).

Our finding that both the *dmnt* loss-of-function alleles resulted in a 24% decrease in life span and a diminished life expectancy was surprising (Fig. 7). Although it is possible that *dmnt* loss of function might have a nonspecific toxic effect, we believe this is unlikely because we fail to observe sensitivity to starvation or bacterial infection in the *dmnt*^{1} mutant flies (Fig. 7; see Fig. S4 in the supplemental material). Nonetheless, we have been unable to demonstrate increased longevity using a dMnt transgene and a motor neuron-specific GAL4 driver used previously to overexpress superoxide dismutase and increase life span (50). However, a negative result with the transgene may well be due to a failure to target expression to the appropriate cell type or developmental time. While this work was in progress, the *mad*/*mnt* homolog, *mdl-1* in *Caenorhabditis elegans* (76) was identified as a positively regulated target of the DAF-16 transcription factor (43), which is known to influence the rate of aging during early adulthood. In addition, *mdl-1* small interfering RNA resulted in a ~10% decrease in the life span of *C. elegans*. Perhaps *D. melanogaster* Mad/Mnt homologs function as part of a conserved pathway involved in longevity. Clearly, further studies will be required to define dMnt's possible role in aging. Interestingly, mammalian c-Myc has been recently shown to have the ability to attenuate cellular senescence and promote transformation through its direct regulation of the Werner syndrome gene, also known to function in aging (22).

Longevity has been closely linked to cell growth pathways in many organisms including *C. elegans*, *D. melanogaster*, and vertebrates (7, 14, 25, 35, 36, 43, 75). We have shown, through dMnt overexpression and loss of function, that this transcriptional repressor has a role in regulating growth. Expression array studies in murine thymocytes containing a Mad1 transgene indicate that Mad downregulates the expression of numerous genes involved in ribosome biogenesis, translation, and metabolism (30). The majority of these repressed genes are activated by Myc. Furthermore, genomic binding studies of dMnt in *D. melanogaster* indicate direct association of dMnt and dMyc proteins with many of the same growth-related genes (48). These findings, taken together with the data reported here, further extend the notion that Myc and Mad/Mnt proteins are antagonists in terms of their transcriptional activities and effects on cell and organismal growth and longevity. It remains to be determined whether *dmnt* is regulated by *Drosophila* FOXO, the only fly homolog of FOXO/DAF-16 (32, 54). If so, dMnt may act to suppress a specific subset of growth-related genes in the absence of insulin and perhaps other growth factors.

ACKNOWLEDGMENTS

We are grateful to Amir Orian, Sara Hook, and Sarah Pierce for critical readings of the manuscript. We also thank Harmit Malik for help and guidance in constructing the phylogenetic tree, Kim McClure for sharing unpublished data, Peter Gallant and Susan Parkhurst for valuable suggestions, the Hybridoma Bank for antibodies, the Bloomington Stock Center for fly stocks, and Gerald Rubin's lab for the fly stocks and dSin3 cDNA.

This work was supported by grants from NIH/NCI (RO1 CA15738 to R.N.E., R01 GM51186 to B.A.E., and F32 GM18246-02 to L.W.M.L.) and the Lady Tata Memorial Trust to J.S. R.N.E. is an American Cancer Society Research Professor.

REFERENCES

1. **Altschul, S. F., T. L. Madden, A. A. Schaffer, J. Zhang, Z. Zhang, W. Miller, and D. J. Lipman.** 1997. Gapped BLAST and PSI-BLAST: a new generation of protein database search programs. Nucleic Acids Res. **25:**3389–3402.
2. **Armstrong, J. A., and B. M. Emerson.** 1998. Transcription of chromatin: these are complex times. Curr. Opin. Genet. Dev. **8:**165–172.
3. **Ayer, D. E., L. Kretzner, and R. N. Eisenman.** 1993. Mad: a heterodimeric partner for Max that antagonizes Myc transcriptional activity. Cell **72:**211–222.
4. **Ayer, D. E., Q. A. Lawrence, and R. N. Eisenman.** 1995. Mad-Max transcriptional repression is mediated by ternary complex formation with mammalian homologs of yeast repressor Sin3. Cell **80:**767–776.
5. **Baudino, T. A., and J. L. Cleveland.** 2001. The Max network gone Mad. Mol. Cell. Biol. **21:**691–702.
6. **Blackwood, E. M., and R. N. Eisenman.** 1991. Max: a helix-loop-helix zipper protein that forms a sequence-specific DNA binding complex with Myc. Science **251:**1211–1217.
7. **Bohni, R., J. Riesgo-Escovar, S. Oldham, W. Brogiolo, H. Stocker, B. F. Andruss, K. Beckingham, and E. Hafen.** 1999. Autonomous control of cell

and organ size by CHICO, a *Drosophila* homolog of vertebrate IRS1-4. Cell **97:**865–875.
8. **Bourbon, H. M., G. Gonzy-Treboul, F. Peronnet, M. F. Alin, C. Ardourel, C. Benassayag, D. Cribbs, J. Deutsch, P. Ferrer, M. Haenlin, J. A. Lepesant, S. Noselli, and A. Vincent.** 2002. A P-insertion screen identifying novel X-linked essential genes in *Drosophila*. Mech. Dev. **110:**71–83.
9. **Brand, A., and N. Perrimon.** 1993. Targeted gene expression as a means of altering cell fates and generating dominant phenotypes. Development **118:** 401–415.
10. **Brown, N. H., and F. C. Kafatos.** 1988. Functional cDNA libraries from *Drosophila* embryos. J. Mol. Biol. **203:**425–437.
11. **Brubaker, K., S. M. Cowley, K. Huang, L. Loo, G. S. Yochum, D. E. Ayer, R. N. Eisenman, and I. Radhakrishnan.** 2000. Solution structure of the interacting domains of the Mad-Sin3 complex: implications for recruitment of a chromatin-modifying complex. Cell **103:**655–665.
12. **Cerni, C., K. Bousset, C. Seelos, H. Burkhardt, M. Henriksson, and B. Luscher.** 1995. Differential effects by Mad and Max on transformation by cellular and viral oncoproteins. Oncogene **11:**587–596.
13. **Chen, J., T. Willingham, L. R. Margraf, N. Schreiber-Agus, R. A. DePinho, and P. D. Nisen.** 1995. Effects of the MYC oncogene antagonist, MAD, on proliferation, cell cycling and the malignant phenotype of human brain tumor cells. Nat. Med. **1:**638–643.
14. **Clancy, D. J., D. Gems, L. G. Harshman, S. Oldham, H. Stocker, E. Hafen, S. J. Leevers, and L. Partridge.** 2001. Extension of life-span by loss of CHICO, a *Drosophila* insulin receptor substrate protein. Science **292:**104–106.
15. **Davis, A. C., M. Wims, G. D. Spotts, S. R. Hann, and A. Bradley.** 1993. A null c-myc mutation causes lethality before 10.5 days of gestation in homozygous and reduced fertility in heterozygous female mice. Genes Dev. **7:**671–682.
16. **de la Cova, C., M. Abril, P. Bellosta, P. Gallant, and L. A. Johnston.** 2004. *Drosophila* myc regulates organ size by inducing cell competition. Cell **117:** 107–116.
17. **Eisenman, R. N.** 2001. Deconstructing myc. Genes Dev. **15:**2023–2030.
18. **Foley, K. P., G. A. McArthur, C. Quéva, P. J. Hurlin, P. Soriano, and R. N. Eisenman.** 1998. Targeted disruption of Mad1 inhibits cell cycle exit during granulocyte differentiation. EMBO J. **17:**774–785.
19. **Gallant, P., Y. Shiio, P. F. Cheng, S. Parkhurst, and R. N. Eisenman.** 1996. Myc and Max homologs in *Drosophila*. Science **274:**1523–1527.
20. **Gehring, S., S. Rottmann, A. R. Menkel, J. Mertsching, A. Krippner-Heidenreich, and B. Luscher.** 2000. Inhibition of proliferation and apoptosis by the transcriptional repressor mad1. Repression of fas-induced caspase-8 activation. J. Biol. Chem. **275:**10413–10420.
21. **Grandori, C., S. M. Cowley, L. P. James, and R. N. Eisenman.** 2000. The MYC/MAX/MAD network and the transcriptional control of cell behavior. Annu. Rev. Cell Dev. Biol. **16:**653–699.
22. **Grandori, C., K. J. Wu, P. Fernandez, C. Ngouenet, J. Grim, B. E. Clurman, M. J. Moser, J. Oshima, D. W. Russell, K. Swisshelm, S. Frank, B. Amati, R. Dalla-Favera, and R. J. Monnat, Jr.** 2003. Werner syndrome protein limits MYC-induced cellular senescence. Genes Dev. **17:**1569–1574.
23. **Grunstein, M.** 1997. Histone acetylation in chromatin structure and transcription. Nature **389:**349–352.
24. **Hartwell, L. H., J. J. Hopfield, S. Leibler, and A. W. Murray.** 1999. From molecular to modular cell biology. Nature **402**(Suppl.)**:**C47–C52.
25. **Hsu, A. L., C. T. Murphy, and C. Kenyon.** 2003. Regulation of aging and age-related disease by DAF-16 and heat-shock factor. Science **300:**1142–1145.
26. **Hurlin, P., C. Queva, and R. N. Eisenman.** 1997. Mnt, a novel Max-interacting protein is coexpressed with Myc in proliferating cells and mediates repression at Myc binding sites. Genes Dev. **11:**44–58.
27. **Hurlin, P. J., K. P. Foley, D. E. Ayer, R. N. Eisenman, D. Hanahan, and J. M. Arbeit.** 1995. Regulation of Myc and Mad during epidermal differentiation and HPV-associated tumorigenesis. Oncogene **11:**2487–2501.
28. **Hurlin, P. J., C. Quéva, P. J. Koskinen, E. Steingrímsson, D. E. Ayer, N. G. Copeland, N. A. Jenkins, and R. N. Eisenman.** 1995. Mad3 and Mad4: novel Max-interacting transcriptional repressors that suppress c-Myc-dependent transformation and are expressed during neural and epidermal differentiation. EMBO J. **14:**5646–5659.
29. **Hurlin, P. J., Z. Q. Zhou, K. Toyo-Oka, S. Ota, W. L. Walker, S. Hirotsune, and A. Wynshaw-Boris.** 2003. Deletion of Mnt leads to disrupted cell cycle control and tumorigenesis. EMBO J. **22:**4584–4596.
30. **Iritani, B. M., J. Delrow, C. Grandori, I. Gomez, M. Klacking, L. S. Carlos, and R. N. Eisenman.** 2002. Modulation of T lymphocyte development, growth, and cell size by the Myc-antagonist Mad1 transcriptional repressor. EMBO J. **21:**4820–4830.
31. **Johnston, L. A., D. A. Prober, B. A. Edgar, R. N. Eisenman, and P. Gallant.** 1999. *Drosophila myc* regulates growth during development. Cell **98:**779–790.
32. **Junger, M. A., F. Rintelen, H. Stocker, J. D. Wasserman, M. Vegh, T. Radimerski, M. E. Greenberg, and E. Hafen.** 7 August 2003, posting date. The *Drosophila* Forkhead transcription factor FOXO mediates the reduction in cell number associated with reduced insulin signaling. J. Biol. **2:**20. [Online.] http://jbiol.com/content/2/3/20.
33. **Koskinen, P. J., D. E. Ayer, and R. N. Eisenman.** 1995. Repression of Myc-Ras co-transformation by Mad is mediated by multiple protein-protein interactions. Cell Growth Differ. **6:**623–629.
34. **Lahoz, E. G., L. Xu, N. Schreiber-Agus, and R. A. DePinho.** 1994. Suppression of Myc, but not E1a, transformation activity by Max-associated proteins, Mad and Mxi1. Proc. Natl. Acad. Sci. USA **91:**5503–5507.
35. **Lee, S. S., S. Kennedy, A. C. Tolonen, and G. Ruvkun.** 2003. DAF-16 target genes that control *C. elegans* life-span and metabolism. Science **300:**644–647.
36. **Leevers, S. J., D. Weinkove, L. K. MacDougall, E. Hafen, and M. D. Waterfield.** 1996. The *Drosophila* phosphoinositide 3-kinase Dp110 promotes cell growth. EMBO J. **15:**6584–6594.
37. **Luscher, B.** 2001. Function and regulation of the transcription factors of the Myc/Max/Mad network. Gene **277:**1–14.
38. **McArthur, G. A., K. P. Foley, M. L. Fero, C. R. Walkley, A. J. Deans, J. M. Roberts, and R. N. Eisenman.** 2002. MAD1 and $p27^{KIP1}$ cooperate to promote terminal differentiation of granulocytes and to inhibit Myc expression and cyclin E-CDK2 activity. Mol. Cell. Biol. **22:**3014–3023.
39. **McArthur, G. A., C. D. Laherty, C. Quéva, P. J. Hurlin, L. Loo, L. James, C. Grandori, P. Gallant, Y. Shiio, W. C. Hokanson, A. C. Bush, P. F. Cheng, Q. Lawrence, B. Pulverer, P. J. Koskinen, K. P. Foley, D. E. Ayer, and R. N. Eisenman.** 1998. The Mad protein family links transcriptional repression to cell differentiation. Cold Spring Harbor Symp. Quant. Biol. **63:**423–433.
40. **McMahon, S. B., H. A. Van Buskirk, K. A. Dugan, T. D. Copeland, and M. D. Cole.** 1998. The novel ATM-related protein TRRAP is an essential cofactor for the c-Myc and E2F oncoproteins. Cell **94:**363–374.
41. **McMahon, S. B., M. A. Wood, and M. D. Cole.** 2000. The essential cofactor TRRAP recruits the histone acetyltransferase hGCN5 to c-Myc. Mol. Cell. Biol. **20:**556–562.
42. **Meroni, G., A. Reymond, M. Alcalay, G. Borsani, A. Tanigami, R. Tonlorenzi, C. L. Nigro, S. Messali, M. Zollo, D. H. Ledbetter, R. Brent, A. Ballabio, and R. Carrozzo.** 1997. Rox, a novel bHLHZip protein expressed in quiescent cells that heterodimerizes with Max, binds a non-canonical E box and acts as a transcriptional repressor. EMBO J. **16:**2892–2906.
43. **Murphy, C. T., S. A. McCarroll, C. I. Bargmann, A. Fraser, R. S. Kamath, J. Ahringer, H. Li, and C. Kenyon.** 2003. Genes that act downstream of DAF-16 to influence the lifespan of *Caenorhabditis elegans*. Nature **424:**277–283.
44. **Neufeld, T. P., A. F. A. de la Cruz, L. A. Johnston, and B. A. Edgar.** 1998. Coordination of growth and cell division in the *Drosophila* wing. Cell **93:** 1183–1193.
45. **Neufeld, T. P., A. Tang, and G. M. Rubin.** 1998. A genetic screen to identify components of the *sina* signaling pathway in *Drosophila* eye development. Genetics **148:**277–286.
46. **Nilsson, J. A., K. H. Maclean, U. B. Keller, H. Pendeville, T. A. Baudino, and J. L. Cleveland.** 2004. Mnt loss triggers Myc transcription targets, proliferation, apoptosis, and transformation. Mol. Cell. Biol. **24:**1560–1569.
47. **O'Neill, E. M., I. Rebay, R. Tjian, and G. M. Rubin.** 1994. The activities of two Ets-related transcription factors required for *Drosophila* eye development are modulated by the Ras/MAPK pathway. Cell **78:**137–147.
48. **Orian, A., B. van Steensel, J. Delrow, H. J. Bussemaker, L. Li, T. Sawado, E. Williams, L. M. Loo, S. M. Cowley, C. Yost, S. Pierce, B. A. Edgar, S. M. Parkhurst, and R. N. Eisenman.** 2003. Genomic binding by the *Drosophila* Myc, Max, Mad/Mnt transcription factor network. Genes Dev. **17:**1101–1114.
49. **Oster, S. K., C. S. Ho, E. L. Soucie, and L. Z. Penn.** 2002. The myc oncogene: MarvelouslY Complex. Adv. Cancer Res. **84:**81–154.
50. **Parkes, T. L., A. J. Elia, D. Dickinson, A. J. Hilliker, J. P. Phillips, and G. L. Boulianne.** 1998. Extension of *Drosophila* lifespan by overexpression of human SOD1 in motorneurons. Nat. Genet. **19:**171–174.
51. **Pierce, S. B., C. Yost, J. S. Britton, L. W. Loo, E. M. Flynn, B. A. Edgar, and R. N. Eisenman.** 2004. dMyc is required for larval growth and endoreplication in *Drosophila*. Development **131:**2317–2327.
52. **Pignoni, F., and S. L. Zipursky.** 1997. Induction of *Drosophila* eye development by Decapentaplegic. Development **124:**271–278.
53. **Poortinga, G., M. Watanabe, and S. M. Parkhurst.** 1998. *Drosophila* CtBP: a Hairy-interacting protein required for embryonic segmentation and hairy-mediated transcriptional repression. EMBO J. **17:**2067–2078.
54. **Puig, O., M. T. Marr, M. L. Ruhf, and R. Tjian.** 2003. Control of cell number by *Drosophila* FOXO: downstream and feedback regulation of the insulin receptor pathway. Genes Dev. **17:**2006–2020.
55. **Pulverer, B., A. Sommer, G. A. McArthur, R. N. Eisenman, and B. Lüscher.** 2000. Analysis of Myc/Max/Mad network members in adipogenesis: inhibition of the proliferative burst and differentiation by ectopically expressed Mad1. J. Cell. Physiol. **183:**399–410.
56. **Queva, C., P. J. Hurlin, K. P. Foley, and R. N. Eisenman.** 1998. Sequential expression of the MAD family of transcriptional repressors during differentiation. Oncogene **16:**967–977.
57. **Queva, C., G. A. McArthur, B. M. Iritani, and R. N. Eisenman.** 2001. Targeted deletion of the S-phase-specific Myc antagonist Mad3 sensitizes neural and lymphoid cells to radiation-induced apoptosis. Mol. Cell. Biol. **21:**703–712.
58. **Rorth, P.** 1996. A modular misexpression screen in *Drosophila* detecting tissue-specific phenotypes. Proc. Natl. Acad. Sci. USA **93:**12418–12422.
59. **Roussel, M. F., R. A. Ashmun, C. J. Sherr, R. N. Eisenman, and D. E. Ayer.**

1996. Inhibition of cell proliferation by the Mad1 transcriptional repressor. Mol. Cell. Biol. **16:**2796–2801.
60. **Rubin, G. M., and A. C. Spradling.** 1982. Genetic transformation of *Drosophila* with transposable element vectors. Science **218:**348–353.
61. **Schreiber-Agus, N., L. Chin, K. Chen, R. Torres, G. Rao, P. Guida, A. I. Skoultchi, and R. A. DePinho.** 1995. An amino-terminal domain of Mxi1 mediates anti-Myc oncogenic activity and interacts with a homolog of the yeast repressor SIN3. Cell **80:**777–786.
62. **Schreiber-Agus, N., Y. Meng, T. Hoang, H. Hou, Jr., K. Chen, R. Greenberg, C. Cordon-Cardo, H.-W. Lee, and R. A. DePinho.** 1998. Role of Mxi1 in ageing organ systems and the regulation of normal and neoplastic growth. Nature **393:**483–487.
63. **Schreiber-Agus, N., D. Stein, K. Chen, J. S. Goltz, L. Stevens, and R. A. DePinho.** 1997. *Drosophila* Myc is oncogenic in mammalian cells and plays a role in the diminutive phenotype. Proc. Natl. Acad. Sci. USA **94:**1235–1240.
64. **Seoane, J., H. V. Le, and J. Massague.** 2002. Myc suppression of the $p21^{Cip1}$ Cdk inhibitor influences the outcome of the p53 response to DNA damage. Nature **419:**729–734.
65. **Seoane, J., C. Pouponnot, P. Staller, M. Schader, M. Eilers, and J. Massague.** 2001. TGFβ influences Myc, Miz-1 and Smad to control the CDK inhibitor $p15^{INK4b}$. Nat. Cell Biol. **3:**400–408.
66. **Staller, P., K. Peukert, A. Kiermaier, J. Seoane, J. Lukas, H. Karsunky, T. Möröy, J. Bartek, J. Massague, F. Hänel, and M. Eilers.** 2001. Repression of $p15^{INK4b}$ expression by Myc through association with Miz-1. Nat. Cell Biol. **3:**392–399.
67. **Stanton, B. R., A. S. Perkins, L. Tessarollo, D. A. Sassoon, and L. F. Parada.** 1992. Loss of N-*myc* function results in embryonic lethality and failure of the epithelial component of the embryo to develop. Genes Dev. **6:**2235–2247.
68. **Stroumbakis, N. D., Z. Li, and P. P. Tolias.** 1994. RNA- and single-stranded DNA-binding (SSB) proteins expressed during *Drosophila melanogaster* oogenesis: a homolog of bacterial and eukaryotic mitochondrial SSBs. Gene **143:**171–177.
69. **Struhl, G., and K. Basler.** 1993. Organizing activity of wingless protein in *Drosophila*. Cell **72:**527–540.
70. **Tatar, M., A. Kopelman, D. Epstein, M. P. Tu, C. M. Yin, and R. S. Garofalo.** 2001. A mutant *Drosophila* insulin receptor homolog that extends life-span and impairs neuroendocrine function. Science **292:**107–110.
70a. **Thompson, J. D., T. J. Gibson, F. Plewnick, F. Jeanmougin, and D. G. Higgins.** 1997. The CLUSTAL_X Windows interface: flexible strategies for multiple sequence alignment aided by quality analysis tools. Nucleic Acids Res. **25:**4876–4882.
71. **Toyo-oka, K., S. Hirotsune, M. J. Gambello, Z. Q. Zhou, L. Olson, M. G. Rosenfeld, R. Eisenman, P. Hurlin, and A. Wynshaw-Boris.** 2004. Loss of the Max-interacting protein Mnt in mice results in decreased viability, defective embryonic growth and craniofacial defects: relevance to Miller-Dieker syndrome. Hum. Mol. Genet. **13:**1057–1067.
72. **Trumpp, A., Y. Refaeli, T. Oskarsson, S. Gasser, M. Murphy, G. R. Martin, and J. M. Bishop.** 2001. c-Myc regulates mammalian body size by controlling cell number but not cell size. Nature **414:**768–773.
73. **Vervoorts, J., J. M. Luscher-Firzlaff, S. Rottmann, R. Lilischkis, G. Walsemann, K. Dohmann, M. Austen, and B. Luscher.** 2003. Stimulation of c-MYC transcriptional activity and acetylation by recruitment of the cofactor CBP. EMBO Rep. **4:**484–490.
74. **Wechsler, D. S., C. A. Shelly, C. A. Petroff, and C. V. Dang.** 1997. MXI1, a putative tumor suppressor gene, suppresses growth of human glioblastoma cells. Cancer Res. **57:**4905–4912.
75. **Weinkove, D., T. P. Neufeld, T. Twardzik, M. D. Waterfield, and S. J. Leevers.** 1999. Regulation of imaginal disc cell size, cell number and organ size by *Drosophila* class I(A) phosphoinositide 3-kinase and its adaptor. Curr. Biol. **9:**1019–1029.
76. **Yuan, J., R. S. Tirabassi, A. B. Bush, and M. D. Cole.** 1998. The *C. elegans* MDL-1 and MXL-1 proteins can functionally substitute for vertebrate MAD and MAX. Oncogene **17:**1109–1118.
77. **Zhou, Z. Q., and P. J. Hurlin.** 2001. The interplay between Mad and Myc in proliferation and differentiation. Trends Cell Biol. **11:**S10–S14.